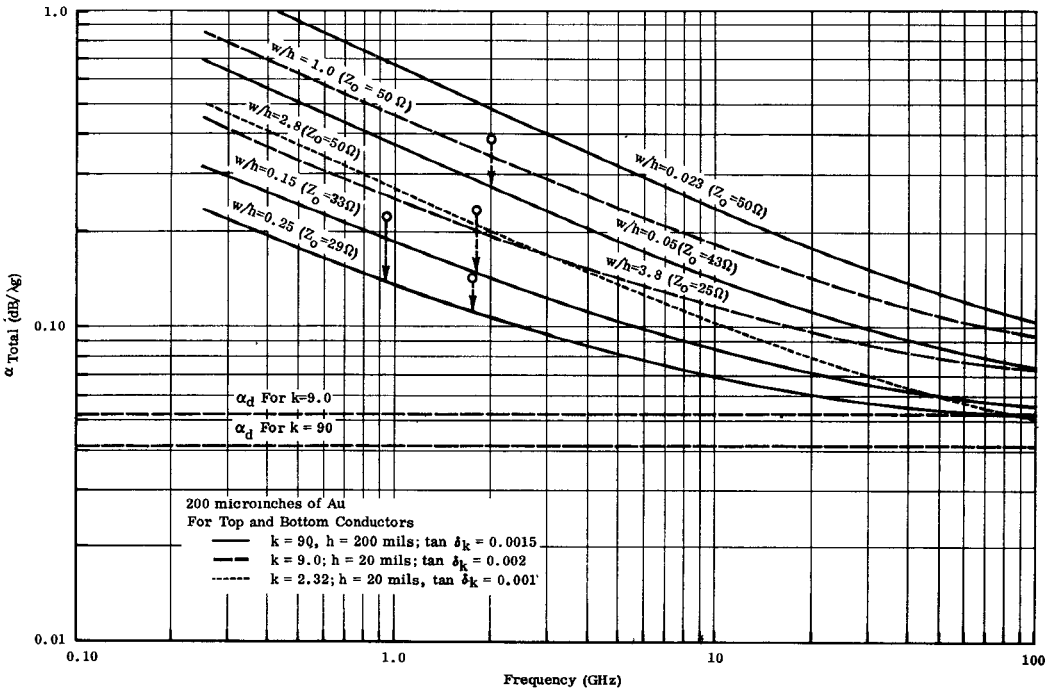

Fig. 3. Attenuation constant versus frequency and geometry.

computed from a conformal mapping solution given by Wheeler.[4]

$$\lambda_0/\lambda_g = \sqrt{k'} \quad (1)$$

$$k' = 1 + q(k - 1) \quad (2)$$

where

k' is the effective dielectric constant;
k is the substrate dielectric constant;
q is the effective filling fraction.

The measured and calculated characteristic impedance is plotted in Fig. 2 as a function of geometry and dielectric constant. The calculated impedance is based on the conformal mapping solution given by Wheeler.[4] Notice that the high-dielectric substrates require smaller values of w/h for high-impedance levels because of the higher transmission-line capacitance. Since line width is restricted by thin-film technology limitations, thicker substrates will be required for high-dielectric microstrip circuits.

From measuring the total loss tangent, the attenuation constant is given by

$$\alpha = 27.3 \tan \delta \quad (\mathrm{dB}/\lambda_g) \quad (3)$$

where tan δ includes both dielectric and conductor loss. The theoretical attenuation may be computed for a TEM wave. The attenuation constant is the sum of the dielectric losses and the conductor losses.

$$\alpha = \alpha_d + \alpha_c. \quad (4)$$

Dielectric losses must include the effective dielectric constant.[5] At low frequencies, where ohmic losses dominate, the dielectric attenuation constant becomes

$$\alpha_d \cong \frac{\omega}{2} (\mu k)^{1/2} \tan \delta_k (k/k')^{1/2} q \ (\mathrm{Np/m}). \quad (5)$$

Conductor losses may be approximately calculated by assuming a uniform current across the width of the conductor and also assuming that the ground plane current is distributed uniformly under the conductor. When the conductor thickness is greater than the skin depth, the conductor attenuation becomes

$$\alpha_c \cong \frac{\sqrt{\pi f \mu \rho}}{Z_0 w} \quad (\mathrm{Np/m}) \quad (6)$$

where

ρ is the conductor resistivity;
f is the frequency;
μ is the magnetic permeability.

Using the relations above, the theoretical attenuation constant and measured values have been plotted in Fig. 3 as a function of frequency and geometry.

Conclusions

High-dielectric substrates consisting of a temperature-compensated titanium dioxide homogeneous mixture have been shown to have the properties required for reduced-size microwave integrated circuits. The variations of microstrip wavelength, characteristic impedance, and attenuation with geometry and dielectric constant are in good agreement with the theory. The low values of attenuation and guide wavelength make this material particularly attractive for low-loss microwave circuitry.

George D. Vendelin
Semiconductor-Components Div.
Texas Instruments Incorporated
Dallas, Tex.

References

[1] T. M. Hyltin, "Microstrip transmission on semiconductor dielectrics," *IEEE Trans. Microwave Theory and Techniques*, vol. MTT-13, pp. 777–781, November 1965.

[2] B. T. Vincent, Jr., "Ceramic microstrip for microwave hybrid integrated circuitry," presented at the Internat'l Microwave Symp., Palo Alto, Calif., May 16, 1966.

[3] M. Caulton, J. J. Hughes, and H. Sobol, "Measurements on the properties of microstrip transmission lines for microwave integrated circuits," *RCA Rev.*, p. 377, September 1966.

[4] H. A. Wheeler, "Transmission-line properties of parallel strips separated by a dielectric sheet," *IEEE Trans. Microwave Theory and Techniques*, vol. MTT-13, pp. 172–185, March 1965.

[5] J. D. Welch and H. J. Pratt, "Losses in microstrip transmission systems for integrated microwave circuits," *NEREM Rec.*, vol. 8, pp. 100–101, 1966.

A Thin-Film *X*-Band Varactor Quadrupler

***Abstract*—A thin-film single idler varactor quadrupler which uses microstrip transmission-line circuitry on ceramic substrate and an unpackaged beam lead varactor are described. Circuit design and the resulting microstrip pattern are discussed; experimental data are presented. Multiplier construction, including information concerning the beam lead varactor and the techniques for bonding it in the circuit pattern, is discussed.**

Manuscript received May 17, 1967; revised September 11, 1967. The work reported here was supported by the Research and Technology Div., Avionics Lab., AF Systems Command under Contract AF 33(615)-2525.

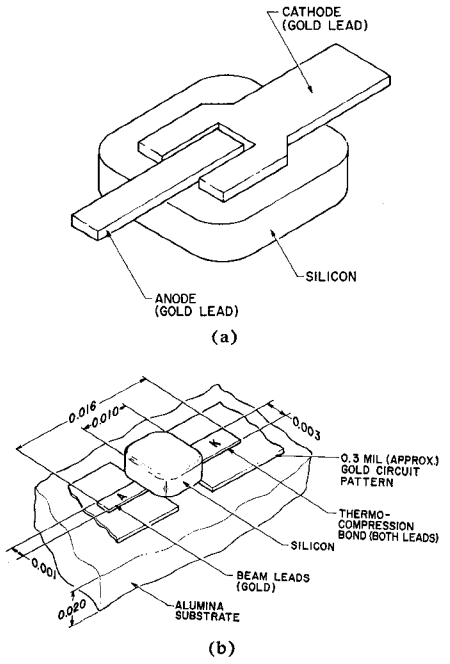

Fig. 1. (a) Typical configuration of the beam lead varactor. (b) Beam lead varactor mounting scheme showing typical dimensions. Note: all dimensions are in inches unless otherwise indicated.

Microwave integrated circuit components continue to be reported and in many applications have exhibited performance equal to or exceeding existing conventional components. Most of these components fall into the category of single frequency band operation, as is normal for phase shifters, mixers, amplifiers, T–R switches, etc., and single values for wave propagation factor and transmission-line loss are adequate for design parameters. Multiplier operation involves two or more frequency bands and consequently poses the additional problems of treating the propagation medium and its microwave circuitry losses over a large frequency range. In microstrip transmission line this problem is particularly severe because of an apparent variation of the velocity of propagation factor as a function of frequency as well as impedance. This effect has been characterized for ceramic substrate by Vincent,[1] and results indicate that it can be minimized by choosing impedance of 50 ohms or greater. Circuit losses increase rapidly as a function of wavelength, however, and can be minimized only by keeping microstrip line lengths to a minimum. It follows from these considerations that multiplier designs, in particular the multifrequency circuits such as shorted stubs, etc., should contain microstrip lines of 50 ohms or greater where feasible, and should be of minimum length, especially for higher frequencies.

A second and equally important consideration for integrated circuit multiplier design, as well as other components, is the technique of mounting the active device, or varactor, in the circuit pattern. For ceramic substrate, shunt mounting is often impractical because

[1] B. T. Vincent, "Ceramic microstrip for microwave hybrid integrated circuitry," presented at the Internat'l G-MTT Symp., Palo Alto, Calif., 1966.

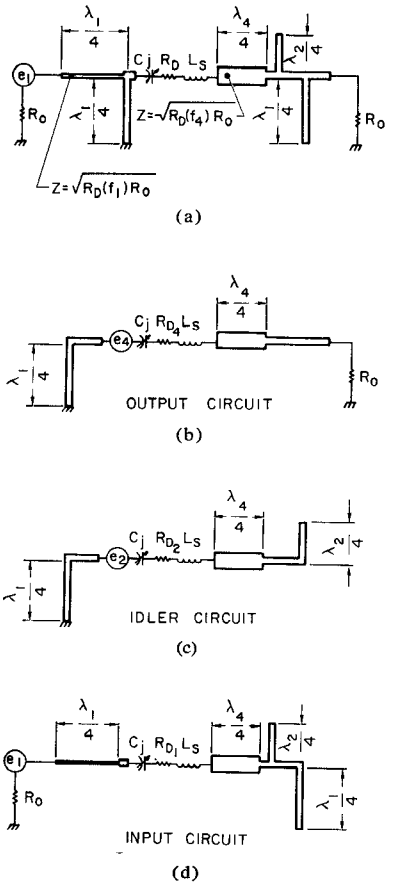

Fig. 2. Schematic diagram of a 2.125 to 8.500 GHz thin-film quadrupler.

of difficulties in drilling holes in the ceramic, and series connection in the circuit pattern is dictated. A beam lead varactor is the logical choice of varactor style for this mounting scheme primarily because of the ease with which it can be bonded into the circuit pattern. Other pertinent factors involved in using the beam lead device include reduction of parasitic device parameters and the ability to replace varactors without destroying the circuit pattern.

Based on the above design considerations, a beam lead varactor suitable for frequency multiplication from S to X band was designed and fabricated. Topside configuration of the varactor is shown in Fig. 1(a); typical dimensions and mounting scheme in microstrip circuitry are shown in Fig. 1(b). Nominal device parameters are $\gamma=0.45$, $V_b=26$ volts, $R_s<2$ ohms, and $f_{c0}=200$ GHz at -6 volts bias.

Fig. 2 shows the schematic diagram for a 2.125 to 8.500 GHz quadrupler designed using the preceding beam lead varactor characteristics. Resonate quarter wavelength microstrip transmission lines are used as filters; interconnecting transmission lines form matching transformers and provide circuit tuning.

Open and shorted stub transmission lines and interconnecting lines are 50 ohms impedance where practical. Transformers are provided by quarter wavelength transmission lines with impedance determined by $Z_t=\sqrt{R_dR_0}$, where R_d is the effective real impedance of the varactor and R_0 is the terminating load. The resulting output, idler, and input circuit representations, for center frequency only, are shown in Fig. 2(b), (c), and (d), respectively. For the purpose of circuit design, measured values of C_j were used and L_s was calculated. The effective real impedance of the varactor R_d was determined initially from theory and tables published by Burkhardt[2] and later optimized experimentally. Initial circuit design was established by series resonating each of circuits shown in Fig. 2 at center frequency. Circuit evaluation at frequencies other than center frequency was made with a laboratory computer program which provided impedance variation as a function of frequency on a Smith chart display. This technique was particularly useful in evaluating circuit design for optimum bandwidth and determining values of R_d and L_s from experimental data.

Fig. 3(a) and (b) shows the unfolded and folded multiplier circuit fabricated on 0.020 inch unglazed alumina (ceramic) substrate which has a dielectric constant of approximately 9.6. Conductor patterns are formed using tantalum–chromium–gold microstrip lines approximately 0.3 mil thick. Varactor mounting is accomplished by thermo-compression bonding the varactor leads on the circuit pattern, with the varactor "inverted" as shown in Fig. 3(c). Physical size of the unfolded model is 0.940 by 0.950 inch. The folded model is 0.550 by 0.830 by 0.040 inch, which includes 0.150 inch added to the circuit width to accommodate system interconnections. Bias circuitry is composed of a low-pass filter network and a bias voltage dropping resistor. The resistor is fabricated on 0.010 inch silicon and attached to the primary substrate.

Experimental data are presented in Figs. 4 and 5. Conversion loss of the unfolded model for 2.125 to 8.500 GHz frequency conversion is <5.9 dB at 10 mW power input, decreases to 5.2 dB at 100 mW input, and is 5.4 dB at 225 mW drive. Input VSWR is less than 1.5 to 1 for the total variation of input power when the varactor bias is optimized for each power level. The 3 dB conversion loss bandwidth is slightly less than 5 percent with maximum input VSWR 1.6 to 1. Spurious harmonics at the output were found to be >40 dB below the output signal for the third and fifth harmonics and >30 dB for the fundamental and second harmonic. For fixed bias operation, all harmonics were >20 dB below the output signal over 2 percent bandwidth.

Experimental data for the folded model shown in Fig. 3(b) have been typically the same as for the unfolded model although further circuit optimization resulted in a decrease in conversion loss. Minimum conversion loss was found to be 4.2 dB (38 percent efficiency) at 225 mW input power.

In summary, the design and construction of the thin-film X-band quadrupler described here offers one approach to multiplier fabrication on ceramic substrate. Although the quadrupler design presented is limited by its

[2] C. B. Burkhardt, "Analysis of varactor frequency multipliers for arbitrary capacitance variation and drive level," *Bell Sys. Tech. J.*, pp. 675–692, April 1965.

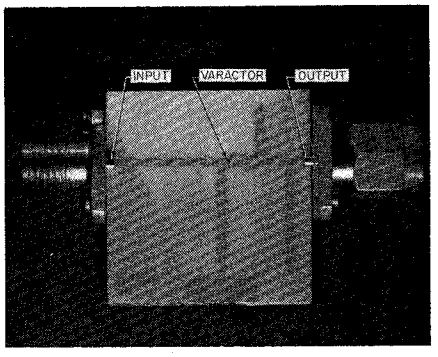

(a)

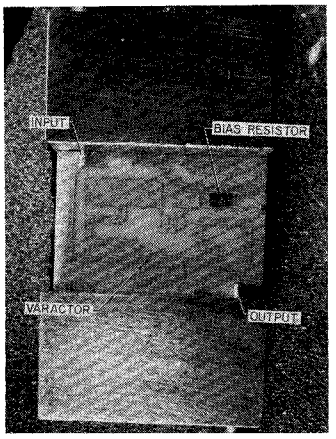

(b)

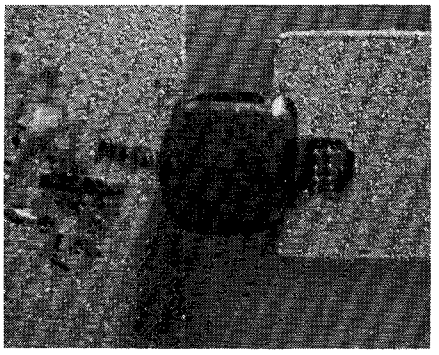

(c)

Fig. 3. (a) The 2.125 to 8.500 GHz quadrupler—unfolded model. (b) The 2.125 to 8.500 GHz quadrupler—folded model. (c) The beam lead varactor mounted in microstrip.

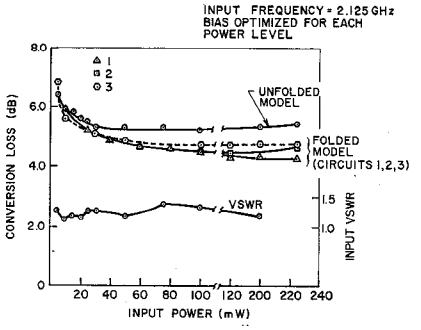

Fig. 4. Input VSWR and conversion loss versus input power for four quadrupler circuits.

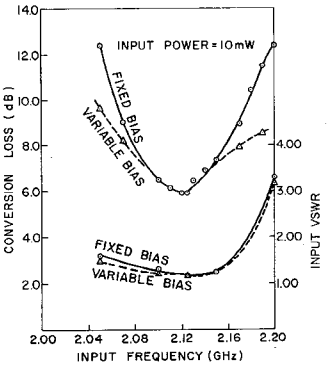

Fig. 5. Input VSWR and conversion loss versus frequency for 10 mW input power.

narrow bandwidth, the feasibility of building quadruplers with reasonable conversion efficiency using microstrip integrated circuit fabrication techniques has been demonstrated. The use of beam lead varactors has contributed significantly to this success.

ACKNOWLEDGMENT

The author wishes to acknowledge the contribution of B. T. Vincent, who was responsible for the design and fabrication of the beam lead varactors.

JOHN B. HORTON
Texas Instruments Incorporated
Dallas, Tex. 75222

Cooling of Avalanche Diodes

This correspondence presents the experimental results of cooling reverse-biased p–n junctions operating in an avalanche transit time mode, and is an extension of previous efforts where the generation and amplification of microwave energy was obtained from conventional varactor diodes.[1]–[4] These are commercially available epitaxial GaAs and Si varactors. The diodes were originally designed for operation as either low-noise parametric amplifiers or harmonic generators. Typically, the diodes exhibit breakdown voltages in excess of 25 volts and junction capacitances less than 1 pF at zero bias.

Basically, the experiment consists of immersing a cold finger attached to the diode through the waveguide mount into a reservoir of liquid nitrogen. Performance was then measured in a *Ku*-band system.

The microwave mount used for these experiments is shown in Fig. 1. It consists of a split guide design insulated at both corners and flange faces when connected to the waveguide system.[5] The diode is mounted on a variable diameter post to which a copper cold finger is attached. The dc bias is directly applied to the diode by means of the bias posts, eliminating the need of coaxial circuitry featuring folded chokes and bypass capacitors to prevent RF leakage. This design has been used extensively as a waveguide circuit for CW operated avalanche transit time devices at this Laboratory.

The dependence of RF output power on reverse-bias current is illustrated in Fig. 2. These curves represent performance of these devices when cooled and uncooled. Because of poor thermal resistance and junction heat sinking, the bias levels of uncooled GaAs units were limited to 10 mA (typically 500 A/cm^2) to prevent burnout. Cooling had the effect of lowering the junction temperature, thus extending the range of operation in this case by 4 mA. With this increase in operating level, a corresponding increase of RF power from 30 to 50 mW was obtained. The operating range of the Si devices was extended from 30 to 40 mA with a corresponding increase in RF power from 28 to 50 mW. In both the GaAs and Si devices the output power did not appear to saturate at the above levels of operation. It is interesting to note that when the cooled devices were operated at the uncooled current levels, the GaAs oscillator showed a slight decrease in RF power output, and the Si devices showed a slight increase. These results were typical for many devices tested.

A plot of the dc to RF efficiency as a function of reverse-bias current is shown in Fig. 3 for the same operating conditions as Fig. 2. The GaAs oscillator shows a net increase of 20 percent in efficiency from 6.3 to 7.5 percent for the 4 mA increase in current. For less efficient GaAs oscillators, the net increase in efficiency is more dramatic; typically an uncooled diode which is 3 percent efficient at 10 mA will be 6 percent efficient at 15 mA. The Si oscillator showed a 50 percent net increase in efficiency from 1.1 percent at 30 mA to 1.7 percent at 40 mA. Saturation effects are dominant for both devices although the RF power out versus the reverse current of Fig. 2 did not indicate any saturation mechanism.

Cooling also improved the performance of these diodes when operated as avalanche amplifiers. Negative resistance amplification was obtained from both the GaAs and Si diodes when used in a circulator-coupled network which formed a one-port reflection type amplifier. The RF power input versus RF power output is shown in Fig. 4 which illustrates the performance of a cooled and uncooled GaAs device. Although amplification was also obtained from Si devices, the results in terms of noise figure, gain, tunability, and stability were not comparable to the GaAs results. In general, the overall response for the cooled amplifier was superior to the uncooled operation. Several points are of interest on this curve. First, gains in excess of 10 dB are obtainable at 0 dBm input level. The room temperature amplifier yielded 17.8 mW output power for 1 mW input when operated at a reverse current of 9.0 mA. The amplifier was then cooled and the reverse current was raised to 15 mA. Under these new operating conditions the output power increased to 38.0 mW for 1 mW of input power. The second point of interest for local oscillator applications is the input level at which 1 mW of output power can be obtained. For the uncooled amplifier this value corresponds to −38 dBm, and for the cooled device it is −52 dBm. The effects

Manuscript received June 5, 1967; revised August 11, 1967.